Journal of Pharmaceutical and Applied Chemistry
An International Journal

http://dx.doi.org/10.18576/jpac/030309

Synthesis, Characterization, Antimicrobial Evaluation and DFT Calculations of Fe(III), Ni(II) and Cu(II) Complexes of Tridentate ONO Donor Ligand

A. M. Abdel-Mawgoud, Mohamed Ismael and Aly Abdou*

Chemistry Department, Faculty of Science, Sohag University, Sohag 82524, Egypt.

Received: 12 Jul. 2017, Revised: 2 Aug. 2017, Accepted: 7 Aug. 2017.
Published online: 1 Sep. 2017.

Abstract: A series of Fe(III), Ni(II) and Cu(II) complexes had been synthesized with molecular formula of $[Fe(L)(H_2O)_2Cl].2H_2O$, $[Ni(L)(H_2O)].2H_2O$ and $[Cu(L)(H_2O)_3].2H_2O$, where L is a Schiff base ligand was derived by condensation of anthranilic acid with 2-hydroxy-benzaldhyde. Structures of the obtained compounds had been characterized using elemental analyses, UV-Vis., FT-IR, magnetic moment and conductivity measurements. Results proposed octahedral geometry for both of Fe(III) and Cu(II) complexes while Ni(II) complex had a square planar geometry. Density Functional Theory (DFT) calculations were performed to confirm the 3D geometry of the compounds and estimate selected electronic parameters (e.g. chemical potential, hardness and electrophilicity index). Moreover free ligand and its metal complexes had been screened for in-vitro antibacterial (Escherichia coli (G-) and Bacillus cereus (G+)) and antifungal (aspergillus fumigatus) activities in terms of the minimum inhibitory concentration (MIC). Results indicated that biological activity increases with complexation.

Keywords: Fe(III), Ni(II), Cu(II) Complexes, Antimicrobial activity, DFT Calculations, 2-{[(IE)-(2-Hydroxyphenyl Methylene]amino} Benzoic Acid.

1 Introduction

Schiff bases form an interesting class of chelating ligands which finds diverse spectrum of biological, clinical, analytical and industrial applications [1]. Schiff bases complexes play a significant role in cancer treatment, antimicrobial, antiviral, fungicidal reagents and for other biological applications [2]. Metal complexes of nitrogen-oxygen Schiff base chelating agents have been studied extensively due to their pronounced applications in biological, clinical, analytical and pharmacological areas [3]. The chemistry of Schiff bases metal complexes is of interest because these species display a variety of reactivity mode in industry as an anticorrosive material [4,5] in medicine as antibiotics, anti-inflammatory reagents, and also as analytical reagents for spectrophotometric determination of some metal ions [6]. Recently, Schiff base complexes have been used as precursors in nanostructures preparation of the respective metal oxides [7,8,9] Schiff bases have interesting ligation properties due to presence of several coordination sites. The metal complexes formed by the combination of transition metal ion with a potent Schiff base ligand should be more biologically active than the metal salts or the ligand individually [10,11]. The great success in biological applications of Schiff bases and their complexes stimulated the search for the discovery of new antimicrobial reagents with high resistance for many clinically relevant pathogens [12,13] As stating above, transition metals complexes and especially iron (Fe), nickel (Ni) and copper (Cu) have been the focus of attention of researchers through the last decades [10,14].

Thus, the aim of the present work is to synthesis a series of Fe(III), Ni(II) and Cu(II) complexes and to assess their in-vitro antimicrobial activity against selected types of bacterial and fungal cultures, which are common contaminants of the environment in Egypt.

2 Chemicals and apparatus

All chemicals were used as produced without further purification. 2-hydroxy-benzaldhyde, anthranilic acid, Fe(III) Chloride ($FeCl_3.6H_2O$), Ni(II) Nitrate

* Corresponding author E-mail: usa_moh2000@yahoo.com

($Ni(NO3)_2.6H_2O$) and Cu (II) Acetate ($Cu(CH_3COO)_2$. H_2O) were obtained from Sigma-Aldrich Company Ltd. JASCO V-770 UV-Vis. Spectrophotometer.

BRUKER Advance 400 and BRUKER FTIR model 8101 were used for the 1H-NMR and IR spectral measurements, respectively for both ligand and complexes. Conductivity and Magnetic susceptibility measurements of the complexes were carried out using JENWAY conductivity meter model 4320 and Bartington Susceptibility instrument at 289 K, respectively. The stiochiometry of the complexes was determined by applying Job's variation [15,16,17].

2.1 Synthesis of Schiff base ligand and complexes

The Schiff base 2-{[(1E)-(2-hydroxyphenyl)met The Schiff base hylene]amino}benzoic acid, H_2L, ligand was prepared as previously reported[18]; A solution of 2-hydroxy-benzaldhyde (10.0 mmol, 1.22 g in 5.0 ml ethanol) was added drop wise to a solut The Schiff base ion of anthranilic acid (10.0 mmol, 1.37 g in 10.0 ml ethanol) with continuous stirring. Then the mixture was refluxed for 2.0 h under constant magnetic stirring. The formed precipitate was collected by filtration, and re-crystallized from ethanol.

Synthesis of the metal complexes followed a general procedure [15] a solution of the H_2L ligand (2.0 mmol, 0.482 g in 8.0 ml ethanol) was added drop wise to an aqueous solution of the metal salt; [Fe(III) chloride (2.0 mmol, 0.54 g in 8.0 ml H_2O)] or [Ni(II) Nitrate (2.0 mmol, 0.58 g in 8.8 ml H_2O) or Cu(II) acetate (2.0 mmol, 0.398 g in 8.8 ml H_2O)], then the reaction mixture was refluxed under constant magnetic stirring for about 4.0 h. Afterwards, the mixture was evaporated over night. Then, the resulting product was collected by filtration, washed by ethanol and finally re-crystallized from ethanol.

2.2 Characterization of the synthetic compounds

The structure of the prepared compounds was proposed from elemental analysis (C, H and N), molar conductance, FT-IR, electronic spectra in addition to magnetic moment measurements. The stoichiometry of the prepared complexes were determined by applying the spectrophotometric Jobs method of continuous variation [12,19,14].

2.3 DFT modeling

To validate the proposed geometrical structures of the, DFT calculations were performed. Geometry optimization calculations were performed using B3LYP functional with basis sets 6-311G (d,p) for the ligand atoms and LANL2DZ with effective core potential (ECP) for the metal ion [20] as implemented in Gaussian 03 program package [21]. In addition to geometry optimization, electronic chemical descriptors such as frontier molecular orbital occupation of the highest occupied molecular orbital (HOMO) and lowest unoccupied molecular orbital (LUMO), energy gap (ΔE), chemical hardness (μ), electronic chemical potential (η), electrophilicity index (ω), and dipole moment (D), had been estimated.

2.5 In-Vitro antimicrobial activity evaluation

The antimicrobial activity of the free ligand and its corresponding metal complexes were primarily screened against pathogenic bacteria and fungus that are common contaminants of the environment in Sohag, Egypt, and some of which are involved in human and animal diseases, e.g. aspergillus fumigatus, or frequently reported from contaminated soil, water and food substances, e.g. Escherichia coli (G-) and Bacillus cereus (G+). The disc diffusion method [22,23] was followed for the detection of antimicrobial activities.

3 Results and discussion

3.1 Characterization of H_2L ligand

IR spectra showed characteristic band at ≈ 3325, 1710 and 1670 cm-1 due to hydroxyl group -OH, carboxylic -C=O and azomethine -CH=N groups, giving good indication for the condensation between anthranilic acid and 2-hydroxy benzaldhyde to form the H_2L ligand, table (1).

The 1H-NMR spectrum showed characteristic signals at ≈ 10.98 ppm (s, 1H), 10.23 ppm (s, 1H) and 8.88 ppm (s, 1H) which attributed to the -COOH, Ar-OH and -CH=N azomethine proton, respectively, while the aromatic protons were appeared at ≈ 6.99-7.70 ppm (m, 8H).

UV-Vis. of H2L ligand showed absorption bands at λmax ≈ 220 and 298 nm, which can be attributed $\pi \rightarrow \pi^*$ transition corresponding to the non-bonding electron pairs of the azomethine group -CH=N, table (1).

3.2 Structure elucidation of metal complexes

3.2.1. Physicochemical properties and conductivity measurements

The complexes were isolated in a good yield, stable at room temperature, non-hygroscopic and had higher melting point than the bare ligand. The complexes were insoluble in water but soluble in common organic solvents, e.g. acetone and DMF. The molar conductivity values of the complexes were relatively low, indicating the non-electrolytic nature of the isolated complexes, table (2). The results of the microanalysis of the prepared complexes are in good agreement with the calculated values, table (2),

suggested that: the subject ligand acts as bi-negatively tridentate and form complexes in 1:1 molar ratio (metal:ligand), with non-electrolytic nature. The weight loss of the thermal decomposition confirmed the presence of two hydrated water molecule in the case of Fe(III), Ni(II) and Cu(II) complexes. Also, the results confirmed the presence of one, two and three water molecules in the coordination sphere of the Ni(II), Fe(III) and Cu(II) binary complexes, which supported the proposed structure of the complexes.

3.2.2. Spectroscopic Studies

3.2.2.1. IR spectra

Infrared spectra considered a powerful technique to give full information to elucidate the structure of the ligand and its bonding nature with the metal ion. The IR spectra of the isolated complexes were compared with those of the bare ligand in order to determine the coordination sites that may be involved in chelation, table (1). There were some guide peaks in the spectra of the ligands and their complexes, which will be helpful in achieving this target. The position of these peaks is expected to change and new peaks will be appeared upon coordination with the metal ion.

The azomethine group υ(-CH=N) stretching vibration of the H_2L ligand appeared at 1670 cm-1, this band was shifted to lower wave numbers upon coordination, which gave good indication for the participation of the azomethine group (-CH=N) in chelation with the metal ion [24,25]. The hydroxyl group (-OH) appeared at ≈ 3325 cm^{-1} in the free H_2L ligand, disappeared in the complexes, indicates the involvement of oxygen atom from hydroxyl group of both carboxylic and phenolic groups, in the chelation with the metal ion after deprotenation. Thus the IR spectral results provided a strong evidence for the coordination between the H_2L ligand and the metal ions as bi-negatively tri-dentate ligand through phenolic -OH, hydroxyl group of the -COOH after de-protenation and azomethine N. The presence of a broad band above 3400 cm^{-1} in the complexes have been assigned to υ(-OH) stretching vibration of hydrated water molecules. New bands are found in the spectra of the complexes in the regions 520-560 and 420-450, which are assigned to υ(M-O) and υ(M-N) stretching vibrations.

3.2.2.2. Electronic spectra

Electronic UV-Vis. spectra are a valuable tool to draw important information about the structural aspects of the colored molecules. Organic ligands, have absorption bands in the ultraviolet region and in some cases these bands extend to higher wavelength region due to conjugation [26] UV-Vis. of H2L, B and MeB ligands showed absorption bands within λmax ≈ 220-300 nm, due to the π→π* transition, corresponding to the non-bonding electron pairs of the -C=N chromophore in benzimidazole ring or azomethine group -CH=N of H_2L ligand.

Upon coordination with metal ions, changes in the

Table (1). IR spectral data and UV-Vis. spectra; wave length (λ_{max}, nm), the H2L ligand and its complexes

	IR spectral bands				U.Vis. spectra	
	υ (OH)	**υ(CH=N)**	**υ (M-O)**	**υ(M-N)**	**λ_{max}**	**assignment**
H_2L	3325	1670	-----	-----	220	π→π*
					298	n→π*
FeL	3432	1588	521	417	266	n→π*
					338	LMCT
NiL	3428	1572	519	440	275	n→π*
					331	LMCT
CuL	3420	1595	550	434	255	n→π*
					338	LMCT
					448	d-d

Table (2). Physicochemical properties of the H2L ligand and its complexes; color, melting point (m.p, oC), yield (%), conductivity (μv, Ω-1. Cm2. mol-1) and magnetic moment (μeff, B.M)

	Empirical formula (M.wt)	**μ_v**	**$\mu_{eff.}$ (B.M)**	**m.p (ºC)**	**Yield (%)**	**Elementa analysis % found (calculated)**				
						C	**H**	**N**	**Cl**	**M**
H_2L	$C_{14}H_{11}NO_3$ (241)	-----	-----	198-200	90	69.70 (69.71)	4.60 (4.56)	5.81 (5.80)	-----	-----
FeL	$[Fe(L)(H_2O)_2Cl].2H_2O$ (402)	13.01	1.75	> 300	75	41.77 (41.79)	4.26 (4.23)	3.48 (3.48)	8.81 (8.83)	13.87 (13.93)
NiL	$[Ni(L)(H_2O)].2H_2O$ (352)	10.80	Dia	> 300	60	47.77 (47.73)	4.26 (4.12)	3.98 (3.97)	-----	16.68 (16.76)
CuL	$[Cu(L)(H_2O)_3].2H_2O$ (393)	11.30	2.18	> 300	65	42.80 (42.75)	4.87 (4.83)	3.57 (3.56)	-----	16.18 (16.15)

UV-Vis. spectra of the ligand are expected due to the electronic structure modifications. Absorption bands due to intra-ligand, π→π* transition, within λmax ≈ 240-260 nm or ligand-to-metal charge transfer (LMCT) or metal-to-ligand charge transfer (MLCT), within λmax ≈ 300-340 nm, were observed for the metal complexes [27], table (1). All these bands exhibited bathochromic shift when compared with that of the free ligands, confirming the coordination of the -C=N with metal ion [28].

3.2.3 Magnetic moment measurements

The magnetic susceptibility and effective magnetic moment can generally be calculated by using the following relationships :

$$\mu_{eff} = 2.83\sqrt{X_A T} \quad \text{where;} \quad X_A = [X_M - (\text{diamagnetic correction})]$$

$$\text{and} \quad X_M = (X_g Mwt)$$

where X_g is the measured gram magnetic susceptibility, X_M molar magnetic susceptibility before correction, X_A Molar magnetic susceptibility after correction, T is the absolute temperature (K) and μeff is the effective magnetic moment (in Bohr Magneton).

The measured μ_{eff} of Fe(III) complex at room temperature are 1.75 B.M, table (2), which would be attributed to one unpaired electron back to d2sp3 hybridization, suggesting a low spin octahedral geometry for the Fe(III) complex. The diamagnetic character of NiL complex would be attributed to dsp2 hybridization of the Ni(II) center ion corresponding to square planar geometry for the Ni(II) complex [29]. The measured μ_{eff} of Cu(II) complex at room temperature is 2.18 B.M, which would be attributed to low spin octahedral geometry[30].

3.2.4 Stiochiomtry of complexes

The stoichiometry of the complexes was determined by applying spectrophotometric job,s method of continuous variation. The continuous variation curve displayed maximum absorbance at mole fraction $X_{ligand} \approx 0.5$, fig. (1), indicating, the coordination between the metal ion and the H_2L ligand in 1:1 (M:L) molar ratio.It is clear by correlation of the previous data; the subject H_2L ligand chelate with the metal ion in bi-negatively tri-dentate manner through the phenolic -OH, hydroxyl group of the -COOH after de-protenation in addition to azomethine N, forming complexes with 1:1 molar ratio (M:L). The composition assigned to the complexes may therefore be formulated as presented in scheme (1).

3.3 DFT modeling of the ligand and metal complexes

The molecular structure of H_2L ligand and its metal complexes are shown in Fig. (2). Optimization of the metal complexes gave stiochiometry of 1:1 (M:L) ratio for metal ion and H_2L ligand. Fe(III) and Cu(II) complexes gave octahedral geometry as; $[Fe(L)(Cl)(H_2O)_2]$ and $[Cu(L)(H_2O)_3]$, while Ni(II) complex gave four coordinate geometry as; $[Ni(L)(H_2O)]$.

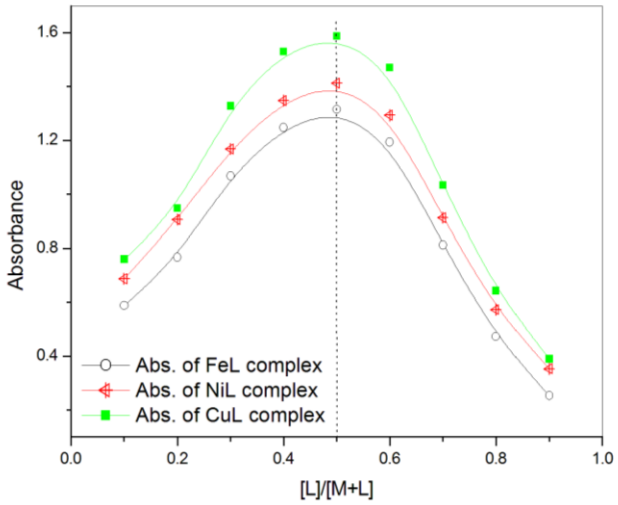

Fig (1). Complex stiochiometry by job method for the prepared complexes

Optimized Frontier molecular orbitals are shown in Fig. (3). For all molecules, the HOMO and LUMO orbitals were delocalized through the whole structure with energy gap less than that of the ligand itself, table (3). The small difference in the energy gap explains the reactivity of the complexes compared with the ligand itself. Furthermore, global electronic descriptors have been estimated for all structures to quantitatively correlate the activity of the molecules with their electronic structure. Those descriptors include chemical hardness (η), electron chemical potential (μ), and electrophilicity index (ω). The later descriptor measure the electrophilic power of the compound which is the change in energy of an electrophile when it comes in contact with a perfect nucleophile.

3.4 Preliminary in-vitro antimicrobial investigation

The free ligand and its corresponding metal complexes have been evaluated against pathogenic bacteria such as Escherichia coli (G-) and Bacillus cereus (G+) and fungus such as aspergillus fumigatus, fig (4) The antimicrobial results revealed that the metal complexes possess notable biological activity than their bare ligand against the selected bacteria/fungi. The activity was greatly enhanced by increasing the concentration. The high activity of the metal chelates than the bare ligand can be explained on the basis of chelation theory [31.32].

Table (3). Calculated HOMO, LUMO, energy gap (ΔE), chemical hardness (η), electronic chemical potential (μ) and electrophilicity (ω) of the H_2L ligand and its corresponding complexes. All values were calculated in eV unit.

Str.	HOMO	LUMO	(ΔE)	(η)	(μ)	(ω)
H_2L	-6.38	-2.31	4.07	2.04	-4.35	4.64
FeL	-6.19	-3.35	2.84	1.42	-4.77	8.01
NiL	-5.90	-2.75	3.15	1.58	-4.33	5.94
CuL	-6.00	-2.53	3.47	1.74	-4.27	5.24

This theory states that chelation reduces the polarity of the metal ion by the partial sharing of its positive charge with donor groups and possible π-electron delocalization over the whole ring. This result in increasing lipophilic character of the complex and favors the penetration of the complex through the lipid layer of cell membrane. The complex may block the binding sites of microorganisms; consequently it disturbs the metabolism pathways or respiration process in the cell, and thus blocks the synthesis of proteins, which restricts further growth of the organism and resulting in the extinction of microorganisms. The complexes activity could be correlated to the strength of the bond between metal and ligand, in addition to size of the cation, receptor sites, diffusion and a joint in fluence of the metal and ligand for inactivation of the biomolecules [33]. The prepared complexes have good biological activity and act as powerful and potent bactereostatic agents, thus inhibiting the growth of bacteria and fungi.

4 Conclusion

The current framework presents the preparation of the H_2L Schiff base ligand and its Fe(III), Ni(II) and Cu(II) complexes. Both the ligand and its complexes were characterized by several physicochemical and spectral analyses to determine their geometry. Moreover, the structural characteristics of H_2L Schiff base ligand and complexes have been investigated using quantum chemical calculations. The antimicrobial screening of the complexes has been examined against the growth of selected pathogenic

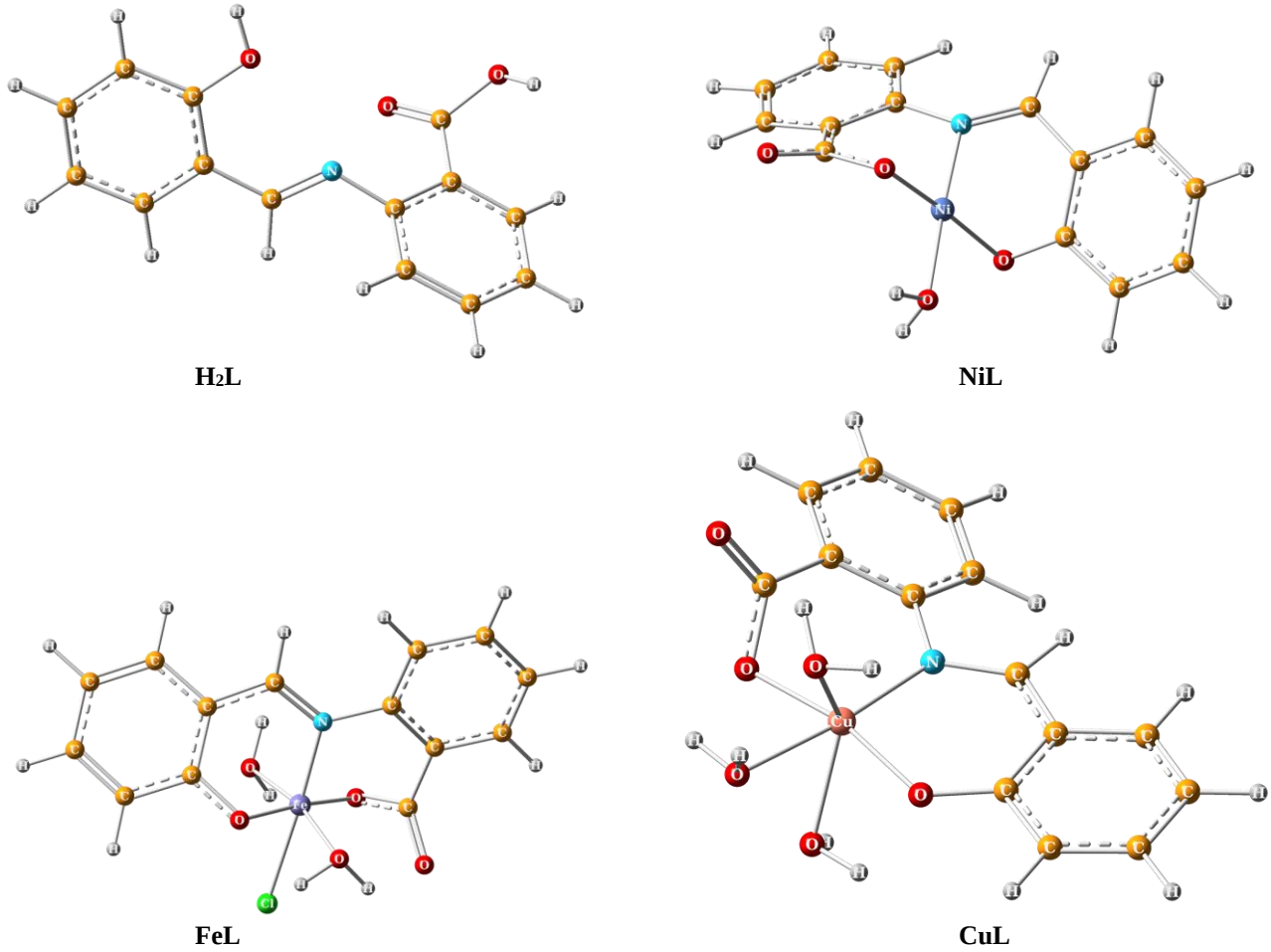

Fig (2). Optimized structures of the H_2L ligand and its metal complexes calculated using DFT method.

bacteria and fungi, e.g. Escherichia coli (G-), Bacillus cereus (G+) and aspergillus fumigatus. The results show that; the complexes exhibited high activity compared to their corresponding Schiff base ligand which indicates that metallization enhances the activity compared of the prepared complexes.

Acknowledgments

The authors gratefully acknowledge Dr. Ahmed El-

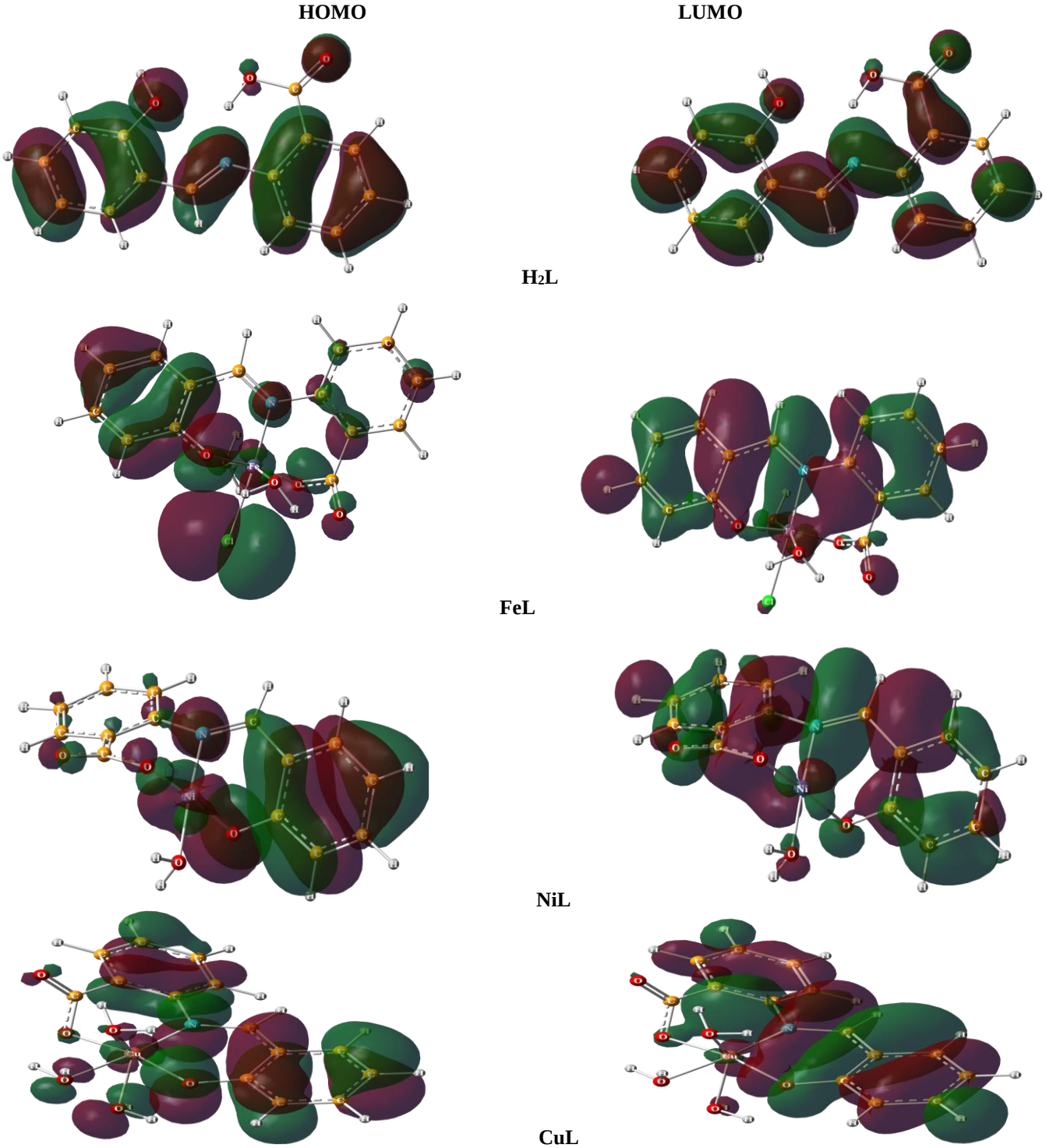

Fig (3). HOMO and LUMO structures of the H_2L ligand and its corresponding metal complexes calculated using DFT method

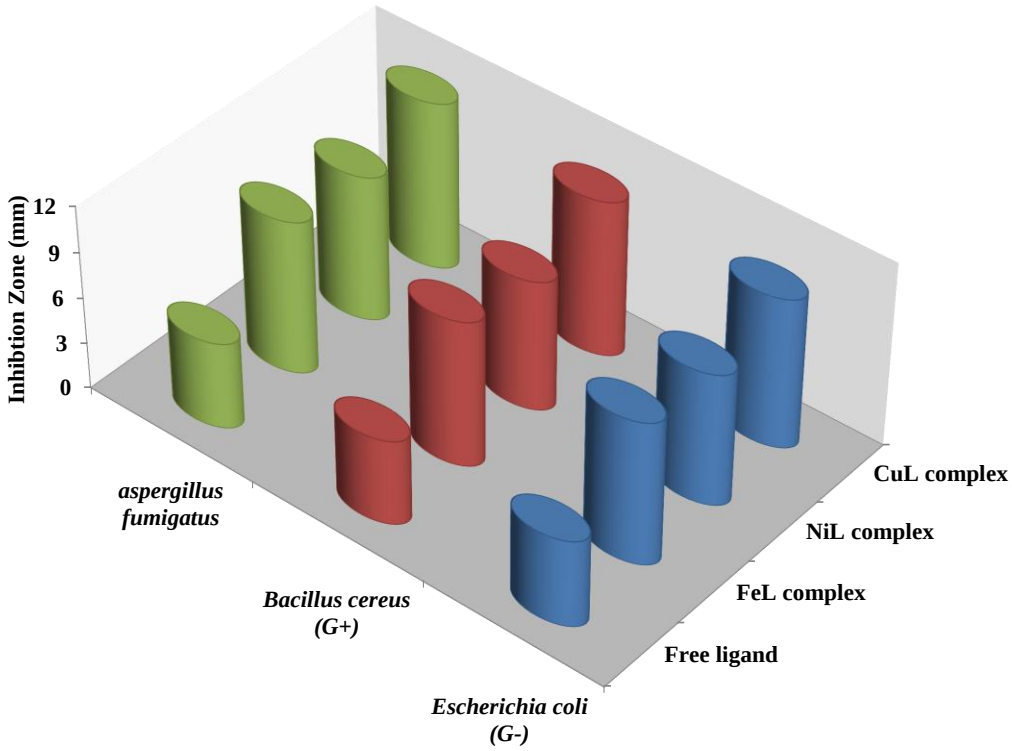

Fig (4). Inhibition zone of the H_2L ligand and its metal complexes.

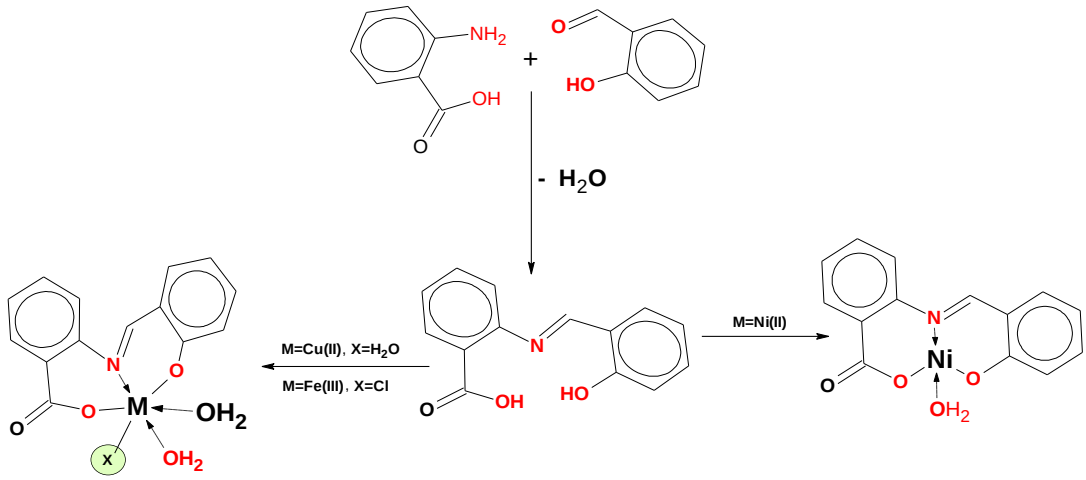

Scheme (1). Structure of the H2L ligand and its metal complexes

Badry, Department of Botany and Microbiology, Faculty of Science, Sohag University, for his helping in antimicrobial activity investigation.

References

[1] A. A. Soayed, H. M. Refaat, D. A. Noor El-Din, Inorganica Chimica Acta, 2013, 406, 230-240.
[2] S. Kumar, D.N. Dhar, P.N. Saxena, J. Sci. Ind. Res., 2009, 68, 181-187.
[3] N. Raman, S. J. Raja, A. Salkthivel, J. Coordination Chemistry, 2009, 62, 691 -709.
[4] J. Liu, B. Wu, B. Zhang, Y. Liu, Turk. J. Chem., 2006, 30, 41-48.
[5] A. Budakoti, M. Abid, A. Azam, Eur. J. Med. Chem., 2006, 41, 63-70
[6] Y. Tachapermpon, S. Chaneam, Adisri Charoenpanich, J. Sirirak, N. Wanichacheva, Sens. Actuator B-Chem., 2017, 241, 868 – 878.
[7] S. Zinatloo-Ajabshir, M. Salavati-Niasari, M. Hamadanian, RSC Adv., 2015, 5, 33792-33800.
[8] S. Mortazavi-Derazkola, S. Zinatloo-Ajabshir, M. Salavati-Niasari, Ceram. Int., 2015, 41, 9593-9601.
[9] S. Mortazavi-Derazkola, S. Zinatloo-Ajabshir, M. Salavati-Niasari, J. Mater. Sci. Mater. Electron., 2015, 26, 5658-5667.

[10] S. O. Podunavac-Kuzmanovic, D. M. Cvetkovic, J. Serb. Chem. Soc., 2007, 72, 459-466.
[11] Shadia A. Galal, Khaled H. Hegab, Ahmed S. Kassab,Mireya L. Rodriguez, Sean M. Kerwin, Abdel-Mo'men A. El-Khamry, Hoda I. El Diwani, Eur J Med Chem, 2009, 44, 1500-1508.
[12] S. K. Bhartia, G. Nathb, R. Tilakb, S. K. Singh, Eur J Med Chem., 2010, 45, 651-660.
[13] M. Singh, S. K. Singh, B. Thakur, P. Ray, S. K. Singh, Anticancer Agents Med Chem., 2016, 16(6) 722-739.
[14] I. Ali, W. A. Wani, A. Khan, A. Haque, A. Ahmad, K. Saleem, N. Manzoor, Microb. Pathog., 2012, 53(2), 66-73.[15] P. Job, Ann. Chem., 1928, 9, 113-203.
[16] R. El-Shiekh , M. Akl, A. Gouda, W. Ali , J. Am. Sci., 2011, 7(4), 797-807.
[17] S. S. Shah, R. G. Parmar, Der Pharma Chemica, 2011, 3(1), 318-321.
[18] Md. R. Hasan, M. A. Hossain, Md. A. Salam, M. N. Uddin, JTUSCI, 2016, 10 (5), 766-773.
[19] R. El-Shiekh, M. Akl, A. Gouda, W. Ali, J. Am. Sci., 2011, 7(4), 797-807.
[20] P.J. Hay, W.R. Wadt, J. Chem. Phys., 1985, 82, 270-283.
[21] M. J. Frisch, G.W.Trucks, H. B. Schlegel, G. E. Scuseria, M. A. Robb, J. R. Cheeseman et al. Gaussian 03, Revision of C.01. Wallingford CT: Gaussian Inc., 2004.
[22] S. O. Podunavac-Kuzmanović, D. M. Cvetković, L. S. Vojinović, APTEFF, 2004, 35, 1-280.
[23] O. A. M. Ali, Spectrochim Acta A Mol Biomol Spectrosc, 2014, 132, 52-60.
[24] K. Singh, R. Thakur, Eur. Chem. Bull., 2016, 5, 193-201.
[25] S. M. Abdallah, M. A. Zayedb, G. G. Mohamed, Arab. J. Chem., 2010, 3, 103-113
[26] R. S. Joseyphus, M. S. Nair, Mycobiology, 2008, 36, 93-98.
[27] S. S. Konstantinovic, B. C. Radovanovic, I. Cakic, V. Vasic, J. Serb. Chem. Soc., 2003, 68, 641-647.
[28] E. N. Md. Yusof, T. B. S. A. Ravoof, E. R. T. Tiekink, A. Veerakumarasivam, K. A. Crouse, M. I. M. Tahir, H. Ahmad, Int. J. Mol. Sci., 2015, 16, 11034-11054.
[29] A. C. E. kennia, D. C. Onwudiwe, L. O. Olasunkanmi, A. A. Osowole, E. E. Ebenso, Bioinorg Chem Appl., 2015, 2015, 789063-12.
[30] P. Antal, B. Drahos, R. Herchel, Z. ľk. Trávníek, Inorg. Chem., 2016, 55 (12), 5957-5972.
[31] M. N. Uddin, D. A. Chowdhury, M. T. Islam, F. Hoque, Orbital Electron. J. Chem., 2012, 4, 273-287.
[32] T. O. Aiyelabola, I. A. Ojo, A. C. Adebajo, G. O. Ogunlusi, O. Oyetunji, E. O. Akinkunmi, A. O. Adeoye, Adv Biol Chem., 2012, 2, 268-273.
[33] A. Fekri, R. Zaky, J. Organomet. Chem., 2016, 818, 15-27.